Journal of Nuclear Materials xxx (2017) xxx-xxx

Contents lists available at ScienceDirect

Journal of Nuclear Materials

journal homepage: www.elsevier.com

Electron and electron-ion sequential irradiation of borosilicate glasses: Impact of the pre-existing defects

Anamul H. Mir[a, *], I. Monnet[b], B. Boizot[c], C. Jégou[a], S. Peuget[a, **]

[a] CEA, DEN, DTCD, SECM, LMPA, BP 17171, 30207 Bagnols-sur-Ceze Cedex, France
[b] CIMAP-GANIL (CEA-CNRS-ENSICAEN-Univ. Caen), BP 5133, 14070 Caen Cedex 5, France
[c] Laboratoire des Solides Irradies, UMR 7642 CEA-CNRS-Ecole Polytechnique, 91128 Palaiseau, France

ARTICLE INFO

Article history:
Received 16 January 2017
Received in revised form 25 March 2017
Accepted 31 March 2017
Available online xxx

Keywords:
Glass
Electron irradiation
Ion irradiation
Raman spectroscopy
Nuclear waste

ABSTRACT

A three-oxide sodium borosilicate glass was irradiated with 2.3 MeV electrons up to 0.15 GGy and 4.6 GGy, and subsequently with 96 MeV Xe ions. The irradiated samples were characterised using Raman spectroscopy, ToF-SIMS, microhardness and surface profilometry. Electron irradiation of the pristine glasses resulted in different structural modifications at the sample surface and in the bulk of the glass, whereas, ion irradiation of either the pristine or bulk of the electron pre-irradiated glasses induced same structural, physical and mechanical property changes. Furthermore, sample surfaces showed a different behaviour than that of the bulk upon subsequent ion irradiation. These results show that the radiation sensitivity of surfaces can significantly vary depending on the type of the irradiation. Therefore, detailed studies aimed at understanding the response of the surfaces to mono and electron-ion double-beam irradiations should be undertaken to address the long-term evolution of the nuclear waste glass matrix surfaces.

1. Introduction

Nuclear waste glass matrices are subjected to self-irradiation damage due to alpha decay (*alpha particle and recoil nuclei*) and beta decay (*electron and gamma*) of the confined radioisotopes. Due to the short half-life time of beta-active radioisotopes, beta decays are dominant only during first few hundred years of the disposal, whereas alpha decays constitute a long-term radiation source. A typical time dependence of the alpha and beta activity and the resulting cumulative dose is shown in Fig. 1(a–d) for a glass confining the nuclear waste coming from the reprocessing of a 33 GWd/tonne fuel burnup in a pressurised water reactor. The intense beta decay, combined with the alpha decay of short-lived Cm^{244} during first few hundred years can result in a glass canister temperature of about 570 K–370 K (*the temperature of the canister varies as a function of the time and radius*) [1]. The cumulative beta-gamma dose saturates at about 5 GGy after a few hundred years *(the saturation dose depends on the initial loading*). Therefore, most of the damage from beta particles will occur at an elevated temperature. On the other hand, alpha decay represents a long-term radiation source. Due to the long half-life time of most of the alpha-active radioisotopes, the dose rate is small – which will not cause any substantial temperature increase. Therefore, the long-term damage from alpha decays will mostly occur at a relatively lower temperature defined by the repository conditions. It is important to bear in mind that the long-term alpha-decay damage will be imposed on a glass matrix already pre-damaged by the electrons from beta-decays. In addition to electron irradiation, the matrices will also be subjected to gamma irradiation at the same time. The dose due to beta particles is about twice the dose due to gamma rays at any point of the time. Because beta and gamma rays cause damage mainly due to ionization, it therefore suffices to address the cumulative ionization damage due to beta-gamma particles using beta particles alone. However, one must stop short of ascertaining that the magnitude of the damage for a given amount of the dose either due to beta particles or gamma rays is the same.

Several studies have been performed in past using actinide-doping, ion, electron and, gamma irradiations on a number of simple and complex glasses to understand the response of the waste matrices to alpha and beta decays. An overview of the effects of various radiations on different glass properties can be found in the following references and the references therein [1–6]. Usually, external ion and electron irradiations are performed on pristine glasses to various dose levels and correlated with the damage evolution of the waste matrices over time. When electron or ion irradiation effects observed in pristine matrices are correlated with beta and alpha-decay damage occurring in the waste matrices, one presumes that any defects introduced by one type of the irradiation do not in any way affect the response of the glass to the other type of the irradiation. In other words, it is assumed that the irradiation response of the pristine glasses is a good representative of the irradiation response of the glasses with pre-existing defects. However, a number of studies have been performed us-

* Corresponding author.
** Corresponding author.
Email addresses: mirinamulhaq@gmail.com (A.H. Mir); sylvain.peuget@cea.fr (S. Peuget)

http://dx.doi.org/10.1016/j.jnucmat.2017.03.047
0022-3115/

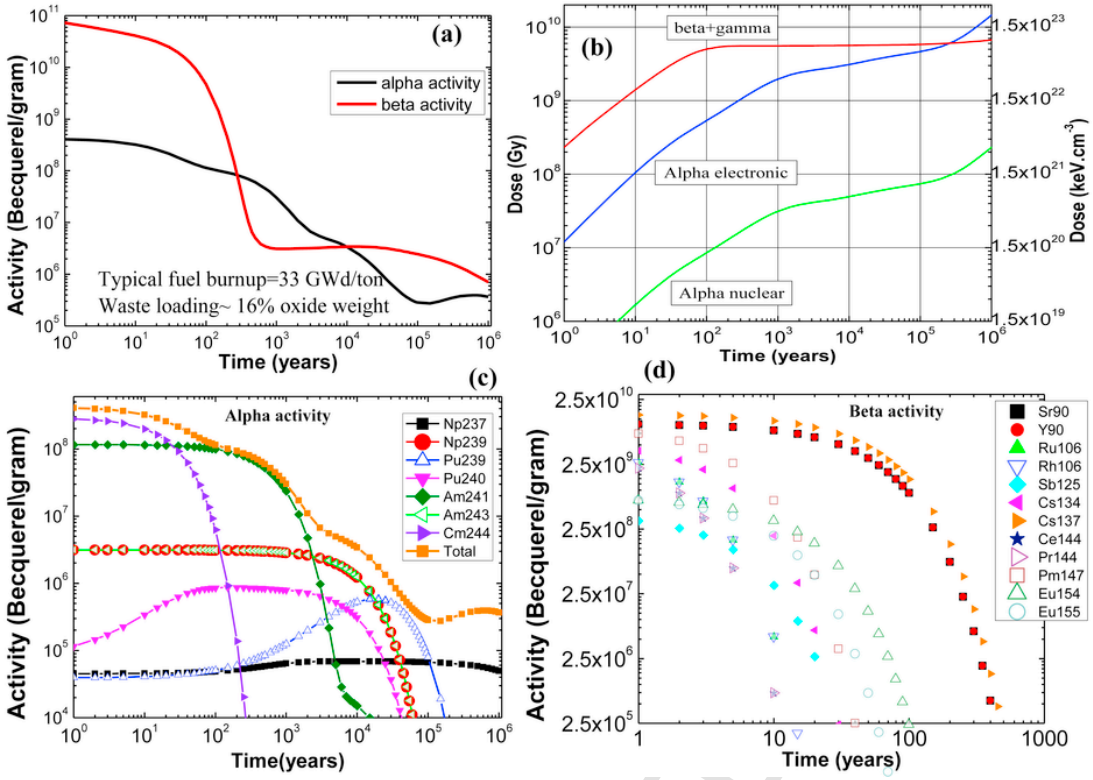

Fig. 1. Radioisotope decay Vs time in a typical nuclear waste glass matrix. (a) Alpha (black) and beta (red) activity over time; (b) Nuclear dose due to alpha decays (green), electronic dose due to alpha decays (blue) and cumulative beta-gamma dose (red) over time. Note that the beta dose is almost twice the gamma dose; (c) activity of the most dominant alpha-active radioisotopes and (d) activity of the most dominant beta-active radioisotopes. The values correspond to a waste derived from a fuel of 33 GWd/tonne burnup and 16% oxide weight waste loading. Note that the saturation beta dose is close to 5 GGy attained in about two hundred years. (For interpretation of the references to colour in this figure legend, the reader is referred to the web version of this article.)

ing multiple beams (*double and triple beams*) [5,7–10] and it has been shown that the defects introduced by one type of irradiation may alter the response of the material to other subsequent irradiations. The combined effect of the electron and ion irradiations (*or the combined effect of alpha and beta decays*) on glass waste matrices has not been studied so far. It is, therefore, important to know if the electron pre-damage can affect the response of the glasses to subsequent alpha decays to better understand the long-term radiation damage in nuclear waste matrices – the aim highlighted in the graphical abstract.

The focus of this work is thus to explore whether electron pre-damage plays any significant role in altering the response of the glasses towards ion irradiation. To address this question, a sodium borosilicate glass (BS3) was irradiated with 2.3 MeV electrons up to 0.15 GGy and 4.57 GGy, and subsequently with 96 MeV Xe^{136} ions to various fluences. The irradiated samples were characterised using Raman spectroscopy, ToF-SIMS, surface profilometry and Vickers microhardness.

2. Experiments

2.1. Samples and irradiation

The composition of the sodium borosilicate glass (BS3) is shown in Table 1. The details about glass preparation can be found elsewhere [11]. Samples of 6 × 6x0.5 mm^3 were optically polished on all the six faces and annealed at about 895 K (*Tg+20*) for 15 min. Annealing was done to remove any stresses due to polishing and reduce the surface roughness to less than 1 nm. The first irradiation was performed with 2.3 MeV electrons at a flux of about 5×10^{13} electrons $cm^{-2}.s^{-1}$ at SIRIUS irradiation facility (*Laboratoire des Solides Irradiés, Ecole Polytechnique, France*) at a temperature of about 350 K (*under a helium atmosphere at 400 mbar*). Homogeneous doses of 0.15 GGy and 4.57 GGy were attained throughout the specimen volume. Following electron irradiation, the samples were irradiated with 96 MeV Xe^{136} ions to various fluences up to a maximum of 4×10^{13} ions.cm^{-2} at GANIL, France (*see* Table 2 *for details*). During ion irradiation, a part of the samples was covered with thick aluminium masks to allow the comparison between ion irradiated and non-irradiated part of the samples. The irradiated samples were characterised using Raman spectroscopy, ToF-SIMS, surface profilometry and Vickers microhardness for accessing structural changes, swelling and hardness variation.

Table 1
BS3 glass composition (weight %).

SiO_2	65.56	Density = 2.45 g cm^{-3} R = 0.8 K = 3.75 Color = transparent Hardness ~6.4 GPa. Tg~875 K
B_2O_3	20.23	
Na_2O	14.21	

2.2. Raman spectroscopy

Horiba HR800 micro-Raman spectrometer using 532 nm excitation laser and 100x objective was used for non-polarized confocal Raman spectroscopy. The depth, lateral and spectral resolutions were 1.6 μm, 1 μm, and 1.7 cm^{-1} respectively. The spectra were acquired

Table 2
Electron and ion irradiation conditions. The stopping power of the ions was calculated using SRIM-2008 (S_e and S_n represent electronic and nuclear energy losses respectively).

Electron dose in GGy. *(2.3 MeV electrons)*	Ion fluence in ions.cm^{-2} *(96 MeV Xe^{136}. S_n =0.1 keV nm^{-1}, S_e =13.5 keV nm^{-1}, Range=12.5 μm, Flux=6x10^9 ions.cm^{-2}.s^{-1}*	Irradiation scenario
0	2×10^{12}, 8×10^{12}, 2×10^{13}, 4×10^{13}	Ion only (i)
0.15	0	Electron only (e)
0.15	2×10^{12}	e + i
0.15	8×10^{12}	e + i
0.15	2×10^{13}	e + i
0.15	4×10^{13}	e + i
4.57	0	e
4.57	4×10^{13}	e + i

on the 6 mm × 6 mm face. A number of spectra were taken in the neighbourhood of a given location to confirm the local damage homogeneity.

2.3. Swelling

For an estimation of the irradiation induced density change, a small portion of the pristine and electron pre-irradiated samples was covered with a thick aluminium foil during Xe^{136} ion irradiation to stop the ion beam within the foil (Fig. 2). As a result of the swelling, a step was formed between the masked and ion irradiated portion of the sample. The step height was measured using Dektak150 surface profiler by scanning across the step. The step height between ion irradiated and pristine part of the samples, and between ion irradiated and electron pre-damaged part of the samples was measured. This permitted to calculate ion, electron, and electron followed by the ion irradiation induced swelling.

2.4. Vickers microhardness

For Vickers hardness measurements, Anton Paar MHT10 system using 50 gf (*0.49 N*) load was used. The indents were observed with Olympus BX51 optical microscope with 100x magnification objective. The value of the hardness was obtained from an average of 25 images (*five indents and 5 images per indent*).

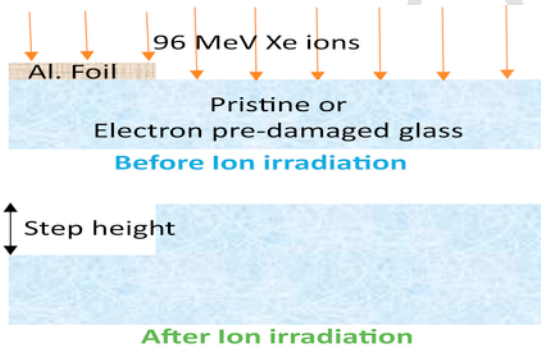

Fig. 2. Xe ion irradiation of pristine or electron pre-irradiated BS3 glass. A thick aluminum foil was used to stop the ion beam from reaching the sample to measure the step height between the pristine and irradiated regions.

2.5. ToF-SIMS

The ToF-SIMS was performed using ToF-SIMS-5 (*ION-TOF, GmbH, Munster, Germany*) at BioPhy, Fuveau. A 200 × 200 μm^2 area was sputtered with 1 keV Cs^+ ions and analysis was performed in an area of 50 × 50 μm^2 using 25 keV Bi_1^+ ions. The profiles were acquired in the centre of the pristine and electron irradiated BS3 glass. More details can be found in Ref. [12].

3. Results

3.1. Raman spectroscopy

3.1.1. Low-dose electron irradiation (0.15 GGy) and subsequent Xe Ion irradiation

Electron irradiation of the pristine BS3 up to a dose of 0.15 GGy did not result in any visible structural changes (Fig. 3). Subsequently, pristine and 0.15 GGy electron pre-irradiated samples were irradiated with 96 MeV Xe^{136} ions to various fluences (Table 2).

The highest fluence case (*4x10^{13} Xe.cm^{-2}*) of the Xe irradiation is shown in Fig. 4. The Raman spectra of the 4×10^{13} Xe.cm^{-2} irradiated BS3 and that of the 0.15 GGy+4×10^{13} Xe.cm^{-2} are very similar. Xenon irradiation caused an increase in the R band position (*which gives an idea about the average Si-O-Si and Si-O-B angles*) by 10 cm^{-1}. The relative intensity of the peak at 630 cm^{-1} decreased (*four-coordinated boron atoms surrounded by three silicon atoms and one boron atom; which is a Danburite like configuration* [13–15]. *Changes in boron co-ordination and local environments of boron and silicon atoms can be inferred from the peaks in this region*). A significant modification was observed in the region from 850 cm^{-1} to 1260 cm^{-1} referred as the Q^n region [10,16,17] (*n represents the number of bridging oxygen atoms, and 0≤n≤4. In a fully polymerised network, each silicon atom is connected to the rest of the glass network through four oxygen atoms called as bridging oxygen atoms*). This region gives an idea about the silica network connectivity. The structural units with a high degree of polymerization contribute towards the high-frequency side of the Q^n region and the units with a low de-

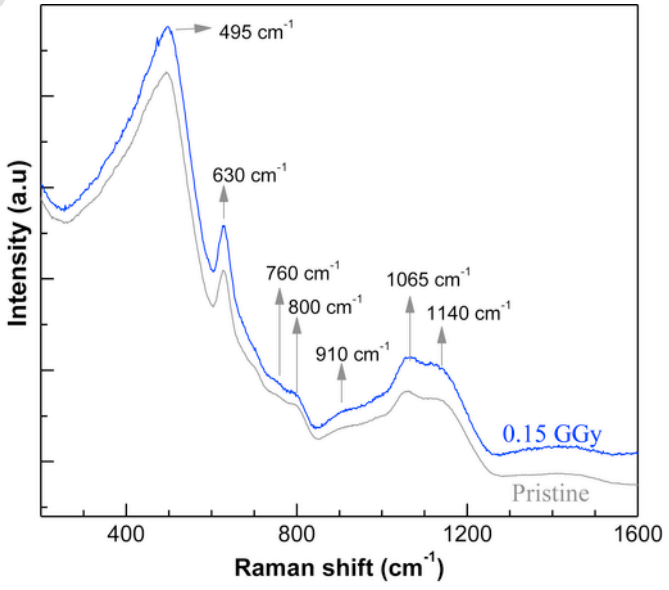

Fig. 3. Raman spectra of the pristine and 0.15 GGy BS3 glass samples.

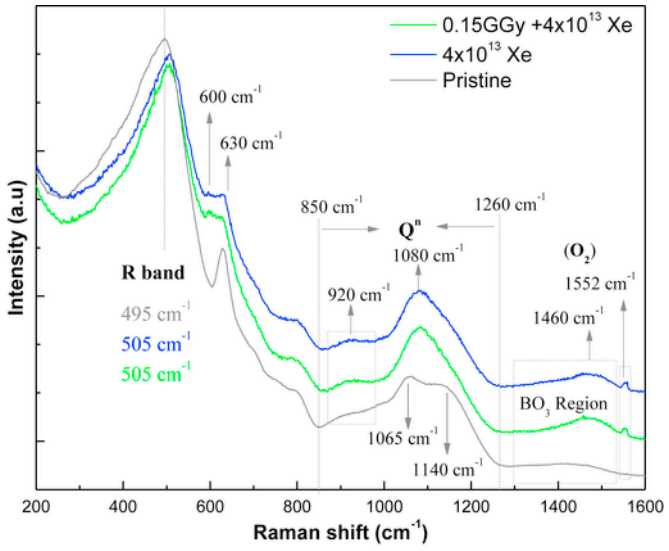

Fig. 4. Raman spectra of pristine, 4×10^{13} Xe.cm^{-2} and 0.15 GGy+4×10^{13} Xe.cm^{-2} samples.

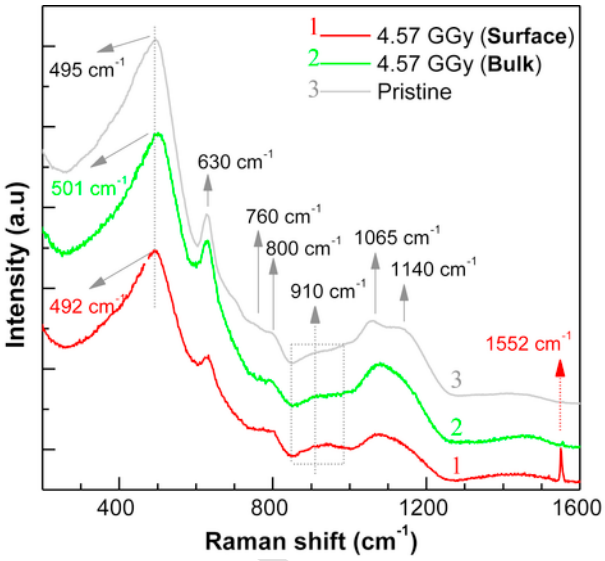

Fig. 5. Raman spectra of the pristine (grey), the surface of the 4.57 GGy (red) and bulk of the 4.57 GGy sample (green). Note that the surface spectrum reflects an average effect in about 1.5 μm depth, whereas the bulk spectrum reflects the behaviour of the sample deep inside and far away from the surface (>2 μm). (For interpretation of the references to colour in this figure legend, the reader is referred to the web version of this article.)

gree of polymerization contribute towards the low-frequency side. A relative decrease in the intensity on the high-frequency side *(> 1140 cm^{-1})*, and an increase in the mid frequency *(>1050 cm^{-1})* and low-frequency side *(<1050 cm^{-1})* indicate a network depolymerization. The region labelled as 'BO_3 region' gives an idea about the proportion of three coordinated boron atoms in the structure. An increase in the intensity of this region, particularly, on the high-frequency side at 1460 cm^{-1} suggests a general increase in the population of the BO_3 units with non-bridging oxygen atoms [18]. In addition, Xe irradiation resulted in the formation of molecular oxygen *(peak at 1552 cm^{-1})*.

A close similarity of the 4×10^{13} Xe.cm^{-2} and 0.15 GGy+4×10^{13} Xe.cm^{-2} cases shows that the electron pre-irradiation at least up to 0.15 GGy does not have any effect on the structural changes induced by the Xe ions (*same was observed at lower Xe fluences. The structural changes due to Xe ion irradiation saturated after irradiation with 8x10^{12} Xe.cm^{-2}*).

3.1.2. High dose electron irradiation (4.57 GGy) and subsequent Xe ion irradiation

A significant structural modification was observed after electron irradiation up to 4.57 GGy. The Raman spectra were acquired on the sample surface (*surface spectra*) and in the bulk (*bulk spectra*) by fracturing the sample in the middle and taking the spectra along the fractured surface (*in addition, a sample was also polished and spectra were taken afterwards*). For depths greater than about 1 μm from the surface, no relative differences were observed in the Raman spectra. However, the structural modifications at the sample surface (*<1 μm region*) were strikingly different from that in the bulk of the glass (*>1 μm region*) (Fig. 5) (*see also* [12] *for more details*). The surface Raman spectra showed a large peak at 1552 cm^{-1} indicating the formation of molecular oxygen (*note that a very small peak was observed after Xe ion irradiation*). No molecular oxygen was observed in the bulk of the glass. The relative intensity of the broad band from 850 cm^{-1} to 960 cm^{-1} (*peaked at 910 cm^{-1} in the pristine*) increased in the surface spectrum. The intensity of the peak at 630 cm^{-1} decreased in the surface spectrum (*a decrease in the danburite like units indicates a decrease in the BO_4 content*) and the position of the R-band decreased by about 3 cm^{-1}, whereas it increased by about 6 cm^{-1} in the bulk (*From many studies one can note that a decrease of $[Na_2O]/[B_2O_3]$ ratio tends to decrease the R band position. Furthermore, a silica-rich phase has always a lower R band position and higher intensity. See for example* [19–21] *for various spectra. Phase separation also tends to decrease the position of the R-band* [19,22]*).*

These results show that the surface and bulk of the glass tend to behave differently. The surface evolves towards an alkali and BO_4 deficient, and molecular oxygen enriched structure with a lower mixing of Si and B atoms.

The sample was subsequently irradiated with 4×10^{13} Xe.cm^{-2}. Due to the structural and composition differences between the surface and bulk, the response to ion irradiation was also different (Fig. 6). Xenon ion irradiation caused a destruction of the molecular oxygen present in the surface layer (*compare 1552 cm^{-1} peak in spectra 1 and 2*). A new peak emerged at 960 cm^{-1} and its origin is uncertain. In the 750 cm^{-1} to 800 cm^{-1} range, the intensity of the region close to 800 cm^{-1} increased, whereas, the intensity close to 760 cm^{-1} decreased (*in borosilicate glasses the bands at 750 cm^{-1} and 770 cm^{-1} are associated with symmetric breathing vibrations of six member rings containing two and one BO_4 tetrahedra respectively* [18,23–26]. *The band near 800 cm^{-1} corresponds to boroxol rings, which are rings of BO_3 units* [27–29]). These results indicate a preferential formation of 3-coordinated boron atoms, particularly the formation of boroxol rings. The relative intensity of the peak at 630 cm^{-1} decreased and a new small peak emerged at 600 cm^{-1}. The position of the R-band decreased by about 2 cm^{-1}. In contrast, the position of the R-band in the bulk increased by about 4 cm^{-1} (*compare spectra 3 and 4*). The relative intensity in the 760 cm^{-1} to 800 cm^{-1} range did not show any significant difference after Xe ion irradiation and no new peak was observed at 960 cm^{-1} in the bulk of the glass. It is important to note that ion irradiation of the pristine (*blue graph in* Fig. 4) and bulk of the electron pre-damaged glasses - irrespective of the dose (*green and pink graphs in* Figs. 4 and 6 *respectively*), resulted in the same final structure.

These changes clearly show that the response of the borosilicate glass surface to external ion irradiation depends on the nature and ex-

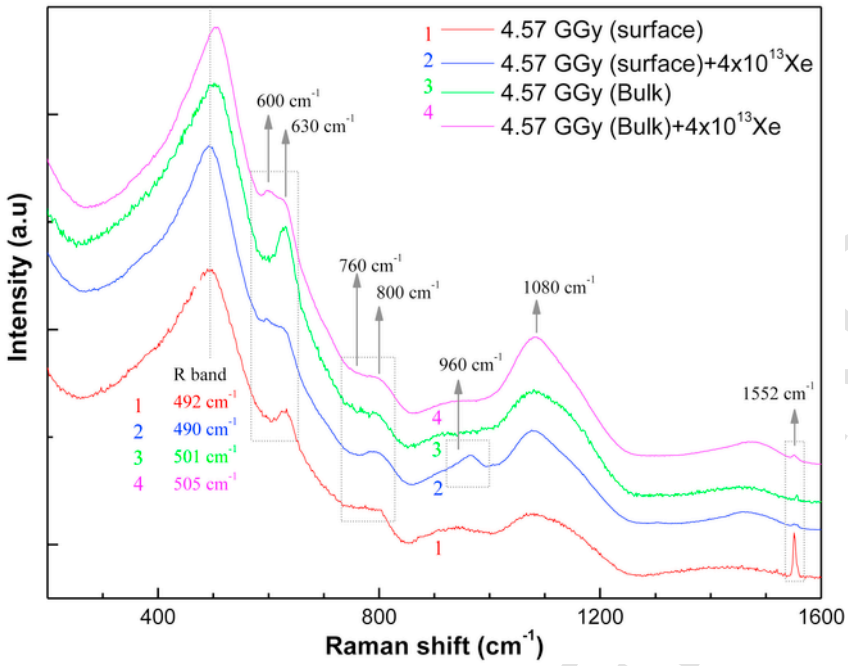

Fig. 6. Comparison of the Raman spectra of electron and electron + ion irradiated glass. Raman spectra after an electron irradiation dose of 4.57 GGy are shown in red (for the surface) and green (for the bulk). The Raman spectra of 4.57 GGy +4 × 13^{13} Xe.cm^{-2} are shown in blue (for the surface) and pink (for the bulk). (For interpretation of the references to colour in this figure legend, the reader is referred to the web version of this article.)

tent of the pre-existing damage due to electron irradiation, whereas, the final state of the bulk of the glass is independent of the pre-existing damage.

3.2. ToF-SIMS

The ToF-SIMS profile of sodium ions obtained in the centre of the pristine and electron irradiated samples is shown in Fig. 7 (*the intensity of the Na^+ was normalised by the intensity of the Si^+ ions*). A depth of about 660 nm was observed to be depleted of the sodium atoms after a dose of 4.57 GGy. No changes were observed in the intensities of boron and silicon atoms. This clearly shows that electron irradiation caused a depletion of sodium atoms from the glass surface. As no structural changes were observed after irradiation with 0.15 GGy, the ToF-SIMS was not performed at this dose level.

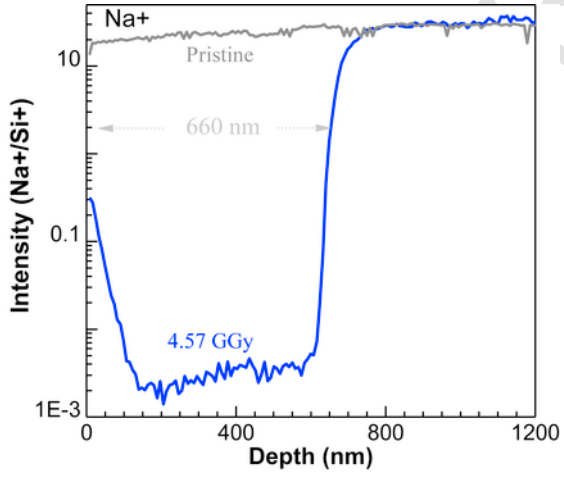

Fig. 7. ToF-SIMS profile of sodium ions in pristine and a sample irradiated with 2.3 MeV electrons up to 4.57 GGy. The profile was taken in the centre of the sample surface (centre of 6 mmx6 mm side). The intensity of the Na ions was normalised by the intensity of silicon ions (more details can be found in Ref. [12].

3.3. Swelling

The swelling induced by the xenon ion irradiation was calculated by measuring the step height between the ion-irradiated and masked part of the sample and dividing it by the range of the Xe ions (*12.5 μm*). This approach assumes that the swelling of first few hundred nanometers of the surface – which was depleted of the sodium atoms, is of the same magnitude as that of the bulk. Maximum step heights of 370 nm, 340 nm and 270 nm (*±10 nm*) were obtained on 4 × 10^{13} Xe.cm^{-2}, 0.15 GGy+4 × 10^{13} Xe.cm^{-2} and 4.57 GGy+4 × 10^{13} Xe.cm^{-2} irradiated samples respectively (Fig. 8a). Thus, the sample with no electron pre-damage showed maximum step height and the one with maximum electron pre-damage showed minimum step height upon Xe ion irradiation. The swelling induced by the Xe ions evaluates to be 3.1%, 2.9% and 2.3% for pristine, 0.15 GGy and 4.57 GGy samples respectively (*shown by the blue bars in* Fig. 8b).

Because the Raman spectra of 4 × 10^{13} Xe.cm^{-2}, 0.15 GGy+4 × 10^{13} Xe.cm^{-2} and 4.57 GGy+4 × 10^{13} Xe.cm^{-2} irradiated BS3 samples are exactly the same (*bulk spectra*), we can, therefore, assume that their swelling level (*with respect to the pristine glass*) is also similar (*~3.1% in all the cases*). Then one can simply calculate the "maximum possible swelling level (~3.1%)" **minus** "swelling during electron-ion sequential irradiation (*which is the step height as shown in* Fig. 8a, *divided by the ion range. This is shown by the blue bars in* Fig. 8b)" to yield the pre-existing swelling due to

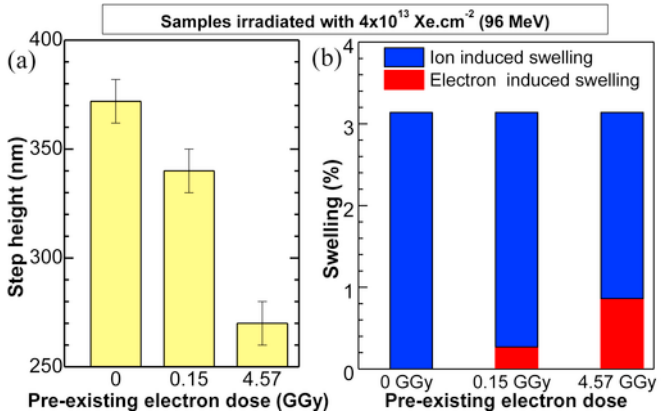

Fig. 8. Step height measurements on pristine and electron pre-irradiated BS3. The swelling was calculated by dividing the step heights by the Xe ion range (~12.5 μm).

electron irradiation. This calculation shows that the electron doses of 0.15 GGy and 4.57 GGy had already induced a swelling of about 0.2% and 0.8% respectively (*shown by the red bars in* Fig. 8b. *This is discussed in more detail in section-4*).

3.4. Vickers micro-Hardness

The hardness was measured on pristine, 0.15 GGy, 0.15 GGy samples irradiated with various Xe ion fluences, 4.57 GGy and 4.57 GGy+4 × 10^{13} Xe.cm^{-2} irradiated samples (*see* Table 2). No change in the hardness was observed after irradiation with electrons up to 0.15 GGy and a hardness decrease of −20 ± 3% was observed after electron irradiation up to 4.57 GGy.

On subsequent ion irradiation, a maximum hardness decrease of −35 ± 3% was observed in the pristine and electron pre-irradiated samples irrespective of the initial electron dose. For the case of pristine and, 0.15 GGy + Xe (*various Xe fluences*), the hardness was observed to saturate after irradiation with 8 × 10^{12} Xe.cm^{-2}. The sample with an initial electron dose of 4.57 GGy was irradiated with a single fluence of 4 × 10^{13} Xe.cm^{-2}. Therefore, the fluence dependence of the hardness for this sample is not known. Thus, one cannot conclude anything about the impact of the pre-existing hardness decrease (*-20% at 4.57 GGy*) on the saturation fluence of the Xe ions.

4. Discussion

4.1. Response of the pristine samples to electron or ion irradiations

As discussed in more details in Ref. [12] and briefly in the current article, the surface of the glass irradiated by 2.3 MeV electrons up to 4.5 GGy tends to evolve towards a phase separated glass with a lower mixing of boron and silicon atoms. This can be attributed to the loss of the sodium atoms from the surface (*~660 nm*) as observed with the ToF-SIMS. On the contrary, the bulk of the glass did not show any tendency towards phase separation after electron irradiation up to 4.57 GGy. From Raman (*current study*) and NMR spectroscopy [12], a slight decrease in the polymerization of the glass network was observed after electron irradiation. In addition, a decrease of the boron coordination and an increase of the non-bridging oxygen atoms around Si and B atoms was observed.

The Xe ion irradiated glass evolved similarly as the bulk of electron irradiated glass but with a higher degree of structural evolution as indicated by the magnitude of the R-band shift and modifications in the Q^n region. Furthermore, a higher degree of swelling and hardness decrease was observed upon ion irradiation in a previous study [3].

4.2. Response of the bulk to electron and subsequent ion irradiation

Raman spectroscopy showed that ion irradiation of the pristine and bulk of the electron pre-irradiated glasses evolved towards the same final state. Therefore, one can conclude that the electron pre-irradiation did not alter the nature of the defect/structural evolution under ion irradiation. The maximum damage was however imposed by the heavy ions (*judging from the extent of the structural variation, hardness decrease and the swelling level*). Since ion irradiation of the pristine and bulk of the electron pre-irradiated glasses resulted in the same final structure and the level of the hardness decrease was also found to be same (*-35%*), therefore, it is plausible to consider that the saturation swelling level was attained during this study and it is same for the pristine and electron pre-irradiated BS3. Although, the degree of swelling (*step height*) from ion irradiation of the electron pre-irradiated glass decreased, it can be simply attributed to the fact that the electron irradiation itself induced a small level of swelling prior to the ion irradiation. Thus, electron and subsequent ion irradiation resulted in an additive damage formation and swelling. Since the maximum level of swelling of the BS3 glass is constant (*a number of studies have shown that BS3 glass shows a maximum swelling of 3.2%* [3,30]*)*, the pre-existing level of swelling due to electron irradiation was calculated to be 0.8% at 4.57 GGy and 0.2% at 0.15 GGy (*note that the maximum ion-induced swelling is about 4 times higher than the maximum electron induced swelling*). It was shown in an earlier study that the structural changes of the BS3 glass saturate after 4.57 GGy [12], therefore, 0.8% represents the maximum level of swelling that electrons can induce in a simple sodium borosilicate glass like BS3. Electrons thus contribute at most 25% to the global swelling. Note that it was assumed that the sodium-depleted region (*~600 nm*) should undergo a similar level of swelling as the bulk of the ion irradiated glass. Therefore, the global level of the swelling does not change. Even if the sodium-depleted region had undergone a different level of swelling, it would not significantly alter the global swelling level owing to its small depth in comparison to the range of the xenon ions (*12.5 μm*).

4.3. Response of the surface to electron and subsequent ion irradiation

The surface of the BS3 glass irradiated up to 4.57 GGy showed significantly different structural modifications relative to the changes in the bulk. A depth of about 660 nm from the surface was depleted of the sodium atoms after irradiation with 4.57 GGy. Due to a loss of the sodium atoms, a significant transformation of BO_4 to BO_3 can be expected to occur in the sodium-depleted region. Such a transformation should increase the local concentration of the non-bridging oxygen atoms (NBO). As a result of the local concentration increase, a certain fraction of the NBO atoms in the depleted region may recombine and result in the formation of molecular oxygen – as observed in the Raman spectra. The changes like decrease in the R-band position and a decrease in the intensity of the peak at 630 cm^{-1} indicate a BO_3 rich surface. As BO_3 has a higher tendency to mix with other BO_3 units [31], this can potentially result in boron rich and silica/borosilicate rich phases on the glass surface. Although there is no direct evidence of any macroscopic phase separation, a decrease in the R-band position is usually observed upon phase separation in borosilicate glasses [19]. Furthermore, high dose electron irradiations using TEMs is well known to result in phase separation and oxygen bubble formation in a number of multi-oxide glasses (*see* Ref. [12] *for de-*

tails). Such studies further support the idea that the sample surfaces in the present study showed a tendency towards boron-silicon demixing.

The effect of ion irradiation on the electron pre-irradiated surface was found to be significantly different from the response of the electron pre-irradiated bulk. Ion irradiation induced a significant decrease of the 630 cm^{-1} peak and an increase in the 800 cm^{-1} peak intensities. Both these changes suggest that ion irradiation tends to drive the surface towards boroxol rich structure (*3-coordinated boron rich*). A further decrease in the R-band position suggests more boron silicon de-mixing due to ion irradiation. Note that heavy ion irradiation of the pristine BS3 has never been observed to result in a decrease of the R-band position so far. Thus, it is purely an effect due to the electron pre-irradiation. In addition, a new peak near 960 cm^{-1} was observed and molecular oxygen disappeared after ion irradiation. The origin of this new peak and the fate of the molecular oxygen is not known at the moment. A possible reason for the disappearance of the molecular oxygen may be associated to its ionization due to high energy Xe ions. Such an ionization effect can lead to the formation of reactive oxygen atoms/radicals which may diffuse through the network faster than the molecular oxygen. Such radicals may, therefore, alter the defect kinetics/evolution during ion irradiation as observed in amorphous silica [9]. The new peak at 960 cm^{-1} is possibly an effect of this complex new reaction mechanism involving oxygen atoms/radicals.

4.4. Long-term response of the nuclear glass waste matrices

Complex glasses like French SON68 – which is closest to the actual French nuclear waste glass R7T7, show a swelling of about 1.3% and 0.6% under heavy ion irradiation [2] and self-irradiation due to alpha decays [2] respectively. If it is assumed that the electrons in such complex glasses cause the same degree of damage as in the simple glass compositions like BS3, then a maximum swelling of about 0.3% can be expected from the electrons (*0.25 × 1.3%*; *assuming a maximum of 25%contribution from electrons as discussed in* section 4.2). However, complex glasses due to the mixed alkali effect and presence of transition metals and lanthanides [32] are usually more resistant to electron irradiation, therefore, 0.3% represents the maximum possible swelling due to electrons in complex glasses like SON68. Ion-induced swelling thus represents the maximum level of swelling nuclear waste matrices can be expected to undergo in the long-term. The dose level of 4.57 GGy is reached almost after 100 years. At this time, the nuclear energy deposition due to alpha-decays should be about 1×10^{20} keV cm^{-3}. At such dose level, nuclear energy induces about 15–20% of the maximum damage level. In a completely additive effect scenario, the global swelling after about 100 years can be expected to be about 40–45% of the maximum swelling level. This assumption however completely ignores the fact that the high glass matrix temperature during the initial phase may cause defect annealing – leading to a recovery phenomenon not observed at low temperatures (*anyway, the electron irradiation in the present study was performed at about 350 K, which is not too low*). Therefore, more studies aimed at addressing this point should be undertaken. In any case, the presence of initial cracks in the glass can easily accommodate such level of expansion without inducing any severe stresses on the canister.

These results highlight that the irradiation sensitivity and behaviour of the surfaces can significantly differ from that of the bulk. A key question is now to evaluate if the structure, properties and response of the electron and electron-ion irradiated surfaces can be regarded as a representative of the radiation damage occurring at the glass-canister interface and surfaces exposed in the cracks. Therefore, further studies addressing the impact of the vacuum (pressure) as well as temperature on the surface alkali depletion phenomenon and its possible impact on the subsequent ion irradiation effects should be undertaken on complex glass compositions. Finally, it is important to highlight that care must be exercised when comparing the chemical reactivity or leaching behaviour of the surfaces with that of the bulk of the externally irradiated glasses as surfaces and bulk tend to have different structures depending on the dose level.

5. Conclusion

Electron and electron-ion sequential irradiations of a sodium borosilicate glass (BS3) were performed with 2.3 MeV electrons and 96 MeV Xe ions to study the effect of the defects created during electron irradiation on the response of the glass to subsequent ion irradiation. The surface, which was found to be depleted of the sodium atoms and enriched in molecular oxygen after electron irradiation, behaved differently than the bulk of the electron-irradiated glass to subsequent ion irradiation. Ion irradiation of the pristine and bulk of the electron pre-irradiated glasses resulted in the same final state irrespective of the pre-existing electron irradiation damage level. After ion irradiation of either the pristine or bulk of the electron-irradiated glass, a swelling of 3.1% and a decrease of glass hardness by −35% was observed. In addition, the Raman spectroscopy showed that the final structural states were same (*glasses were depolymerised*). This shows that the electron irradiation induced defects do not alter the response of the bulk of the glass towards subsequent ion irradiation.

On the other hand, electron irradiation induced defects in the surface region (<1 μm depth) changed the response of the surface towards ion irradiation. The molecular oxygen created during electron irradiation was destroyed upon ion irradiation and the surface showed more tendency towards Si-B demixing.

These results highlight that it is reasonable to correlate the ion irradiation response of either the pristine glasses or bulk of the electron pre-irradiated glasses with the long-term irradiation response of the bulk of the nuclear waste matrices. However, the same is not true for simulating the irradiation response of the exposed surfaces of the waste matrices. Further studies aimed at addressing the relevance of the surface alkali depletion mechanism to the nuclear waste glass matrices should be undertaken. Since the surfaces of the pristine and electron pre–irradiated glasses showed different behaviour upon ion irradiation than their bulk, therefore, to better understand the long-term response of the exposed surfaces, defects due to electron pre-irradiation may need to be considered.

Acknowledgement

This work was supported by the CEA Vestale project. The irradiation experiments were supported by the French EMIR Accelerator network. The authors would like to thank the supporting teams at SIRIUS electron irradiation facility and GANIL-IRRSUD ion irradiation facility.

References

[1] W.J. Weber, Radiation and thermal ageing of nuclear waste glass, Procedia Mater. Sci. 7 (2014) 237–246.
[2] S. Peuget, J.-M. Delaye, C. Jégou, Specific outcomes of the research on the radiation stability of the French nuclear glass towards alpha decay accumulation, J. Nucl. Mater 444 (2014) 76–91, http://dx.doi.org/10.1016/j.jnucmat.2013.09.039.
[3] A.H. Mir, S. Peuget, I. Monnet, M. Toulemonde, S. Bouffard, C. Jegou, Mono and sequential ion irradiation induced damage formation and damage recovery

in oxide glasses: stopping power dependence of the mechanical properties, J. Nucl. Mater 469 (2015) 244–250.
[4] W.J. Weber, R.C. Ewing, C.A. Angell, G.W. Arnold, A.N. Cormack, J.-M. Delaye, D.L. Griscom, L.W. Hobbs, A. Navrotsky, D.L. Price, A.M. Stoneham, M.C. Weinberg, Radiation effects in glasses used for immobilization of high-level waste and plutonium disposition, J. Mater. Res. 12 (1997) 1946–1978. http://discovery.ucl.ac.uk/191727/1/S0884291400040619.pdf.
[5] G. Möbus, G. Yang, Z. Saghi, X. Xu, R.J. Hand, A. Pankov, M.I. Ojovan, Electron irradiation and electron tomography studies of glasses and glass nanocomposites, In: Mater.Res.Soc.Symp. Proc, 2008.
[6] M.I. Ojovan, W.E. Lee, Alkali ion exchange in γ-irradiated glasses, J. Nucl. Mater 335 (2004) 425–432, http://dx.doi.org/10.1016/j.jnucmat.2004.07.050.
[7] L. Thomé, A. Debelle, F. Garrido, S. Mylonas, B. Décamps, C. Bachelet, G. Sattonnay, S. Moll, S. Pellegrino, S. Miro, P. Trocellier, Y. Serruys, G. Velisa, C. Grygiel, I. Monnet, M. Toulemonde, P. Simon, J. Jagielski, I. Jozwik-Biala, L. Nowicki, M. Behar, W.J. Weber, Y. Zhang, M. Backman, K. Nordlund, F. Djurabekova, Radiation effects in nuclear materials: role of nuclear and electronic energy losses and their synergy, Nucl. Inst. Methods Phys. Res. B 307 (2013) 43–48, http://dx.doi.org/10.1016/j.nimb.2012.11.077.
[8] W.J. Weber, E. Zarkadoula, O.H. Pakarinen, R. Sachan, M.F. Chisholm, P. Liu, H. Xue, K. Jin, Y. Zhang, Synergy of elastic and inelastic energy loss on ion track formation in SrTiO3-supplementary data, Sci. Rep. 5 (2015) 1–11.
[9] A.H. Mir, M. Toulemonde, C. Jegou, S. Miro, Y. Serruys, S. Bouffard, S. Peuget, Understanding and simulating the material behavior during multi-particle irradiations, Sci. Rep. 6 (2016) 30191.
[10] A.H. Mir, S. Peuget, M. Toulemonde, P. Bulot, C. Jegou, S. Bouffard, Defect recovery and damage reduction in borosilicate glasses under double ion beam irradiation, Europhys. Lett. 112 (2015) 36002.
[11] C. Mendoza, S. Peuget, T. Charpentier, M. Moskura, R. Caraballo, O. Bouty, A.H. Mir, I. Monnet, C. Grygiel, C. Jegou, Oxide glass structure evolution under swift heavy ion irradiation, Nucl. Inst. Methods Phys. Res. B 325 (2014) 54–65, http://dx.doi.org/10.1016/j.nimb.2014.02.002.
[12] A.H. Mir, B. Boizot, T. Charpentier, M. Gennisson, M. Odorico, R. Podor, C. Jégou, S. Bouffard, S. Peuget, Surface and bulk electron irradiation effects in simple and complex glasses, J. Non-Crystalline Solids 453 (2016) 141–149.
[13] D. Manara, a. Grandjean, D.R. Neuville, Advances in understanding the structure of borosilicate glasses: a Raman spectroscopy study, Am. Mineral. 94 (2009) 777–784, http://dx.doi.org/10.2138/am.2009.3027.
[14] D. Manara, a. Grandjean, D.R. Neuville, Structure of borosilicate glasses and melts: a revision of the Yun, Bray and Dell model, J. Non. Cryst. Solids 355 (2009) 2528–2531, http://dx.doi.org/10.1016/j.jnoncrysol.2009.08.033.
[15] B.G. Parkinson, D. Holland, M.E. Smith, C. Larson, J. Doerr, M. Affatigato, S. a. Feller, a. P. Howes, C.R. Scales, Quantitative measurement of Q3 species in silicate and borosilicate glasses using Raman spectroscopy, J. Non. Cryst. Solids 354 (2008) 1936–1942, http://dx.doi.org/10.1016/j.jnoncrysol.2007.06.105.
[16] P. McMillan, Structural studies of silicate glasses and melts-applications and limitations of Raman spectroscopy, Am. Mineral. 69 (1980) 622–644.
[17] B.O. Mysen, L.W. Finger, D. Virgo, Curve-fitting of Raman spectra of silicate glasses, Am. Minerol. 67 (1982) 686–695.
[18] T. Yano, N. Kunimine, S. Shibata, M. Yamane, Structural investigation of sodium borate glasses and melts by Raman spectroscopy. I. Quantitative evaluation of structural units, J. Non. Cryst. Solids 321 (2003) 137–146, http://dx.doi.org/10.1016/S0022-3093(03)00158-3.
[19] T. Furukawa, W.B. White, Raman spectroscopic investigation of sodium borosilicate glass structure, J. Mater. Sci. 16 (1981) 2689–2700, http://dx.doi.org/10.1007/BF02402831.
[20] A.A. Osipov, L.M. Osipova, Structure of glasses and melts in the Na2O-B2O3 system from high-temperature Raman spectroscopic data: I. Influence of temperature on the local structure of glasses and melts, Glas. Phys. Chem. 35 (2009) 121–131, http://dx.doi.org/10.1134/S1087659609020011.
[21] S.A. Brawer, W.B. White, Raman spectroscopic investigation of the structure of silicate glasses. I. The binary alkali silicates, J. Chem. Phys. 63 (1975) 2421, http://dx.doi.org/10.1063/1.431671.
[22] W.B. White, Investigation of phase separation by Raman spectroscopy, J. Non-Crystalline Solids 49 (1982) 321–329.
[23] R. Akagi, N. Ohtori, N. Umesaki, Structural studies of Na2O–B2O3 glasses and melts using high-temperature Raman spectroscopy, J. Non. Cryst. Solids 293–295 (2001) 471–476, http://dx.doi.org/10.1016/j.physb.2010.08.025.
[24] D. Maniu, I. Ardelean, T. Iliescu, S. Cı^nta, V. Nagel, W. Kiefer, Raman spectroscopic investigations on oxide glass system (1−x)[3B2O3·K2O]·xTiO2, J. Mol. Struct. 480–481 (1999) 657–659, http://dx.doi.org/10.1016/S0022-2860(98)00831-X.
[25] W.L. Konijnendijk, The Structure of Borosilicate Glasses (Thesis), 1975.
[26] D. Maniua, T. Iliescu, I. Ardelean, S. Cinta-Pinzaru, N. Tarcea, W. Kiefer, Raman study on B2O3-CaO glasses, J. Mol. Struct. 651–653 (2003) 485–488, http://dx.doi.org/10.1016/S0022-2860(03)00129-7.
[27] G. Ferlat, T. Charpentier, A. Seitsonen, A. Takada, M. Lazzeri, L. Cormier, G. Calas, F. Mauri, Boroxol rings in liquid and vitreous B2O3 from first principles, Phys. Rev. Lett. 101 (2008) 65504, http://dx.doi.org/10.1103/PhysRevLett.101.065504.
[28] M.A. Kaneshisa, R.J. Elliote, Vibrations of boron oxide glass*, Mater. Sci. Eng. B 3 (1989) 163–166.
[29] W.L. Konijnendijk, J.M. Stevels, The structure of borate glasses studied by Raman scattering, J. Non. Cryst. Solids 18 (1975) 307–331.
[30] A.H. Mir, Radiation Damage in Oxide Glasses: Importance of Energy Deposition and Relaxation Processes, University de Caen, France, 2015.
[31] L. Du, J.F. Stebbins, Nature of silicon-boron mixing in sodium borosilicate glasses: a high-resolution 11B and 17O NMR study, J. Phys. Chem. B 107 (2003) 10063–10076.
[32] N. Ollier, B. Boizot, B. Reynard, D. Ghaleb, G. Petite, Beta irradiation in borosilicate glasses: the role of the mixed alkali effect, Nucl. Inst. Methods Phys. Res. B 218 (2004) 176–182, http://dx.doi.org/10.1016/j.nimb.2003.12.014.